Electronic Supplementary Material (ESI) for Journal of Materials Chemistry A

Electronic Supplementary Information (ESI)

Designed synthesis of hematite-based nanosorbents for dye removal

Junshu Wu, Jinshu Wang*, Hongyi Li, Yucheng Du, Kelin Huang, and Baixiong Liu

School of Materials Science and Engineering, Beijing University of Technology,

Chaoyang District, Beijing 100124, China

Contact address: wangjsh@bjut.edu.cn

Tel/Fax: +861067391101

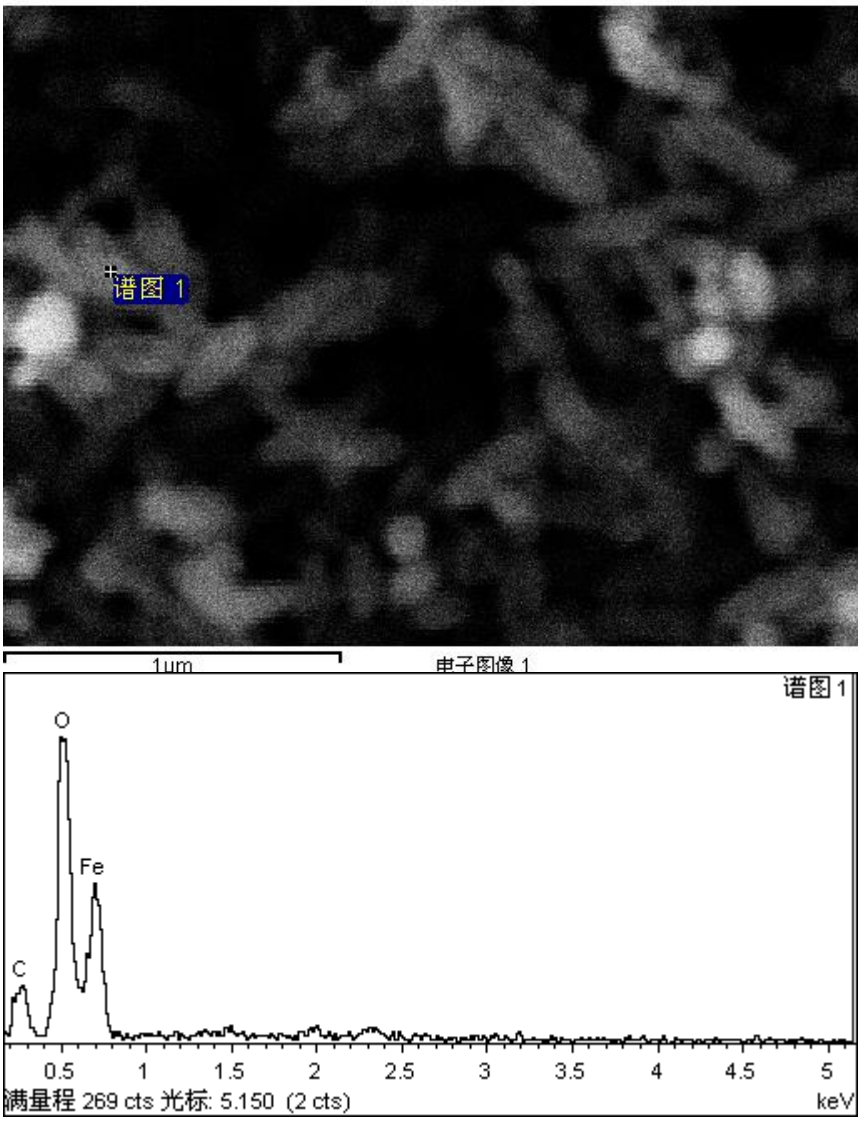

Fig. S1 EDX spectrum of FHSs. The C signal is from carbon conductive tape.

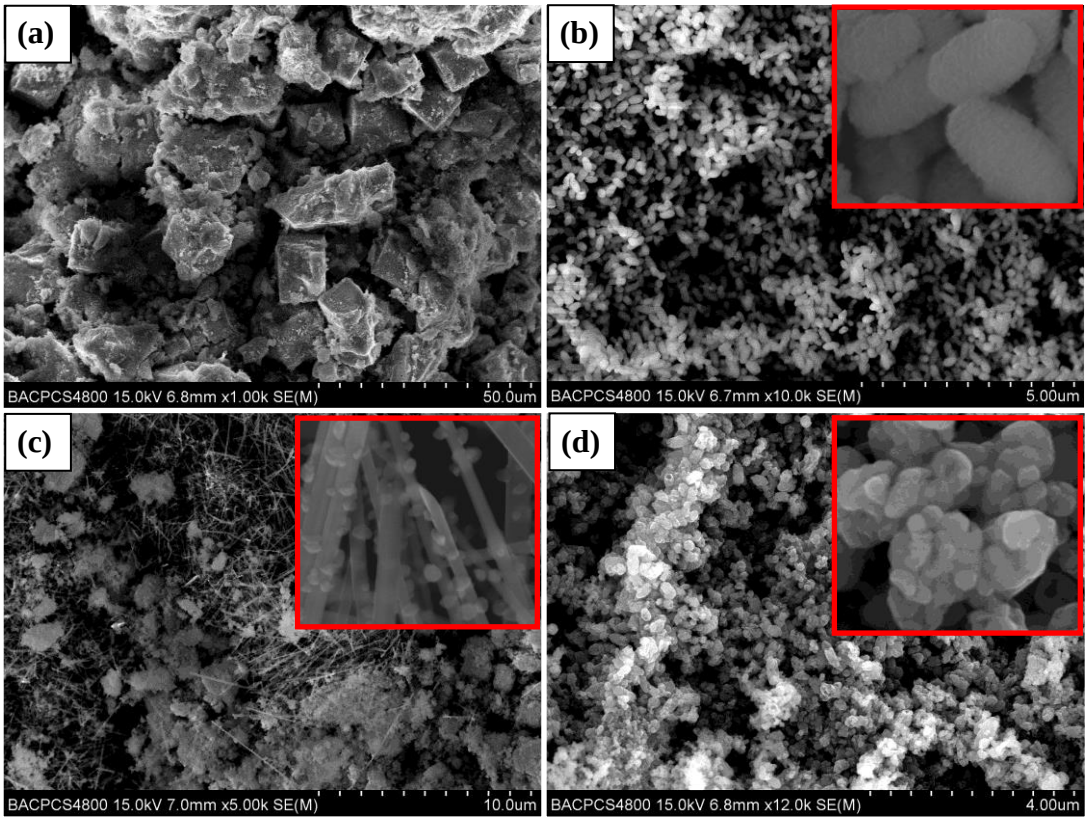

Fig. S2 SEM images of the products obtained by hydrothermal treatment of 0.05 g KW in 10 mL 0.2 M $Fe(NO_3)_3$ aqueous solution (170–180 °C, 36 h) with the addition of (a) 0.3 g SDBS, (b) 0.2 g SDBS, (c) 0 g SDBS, (d) 0.086g SDS.

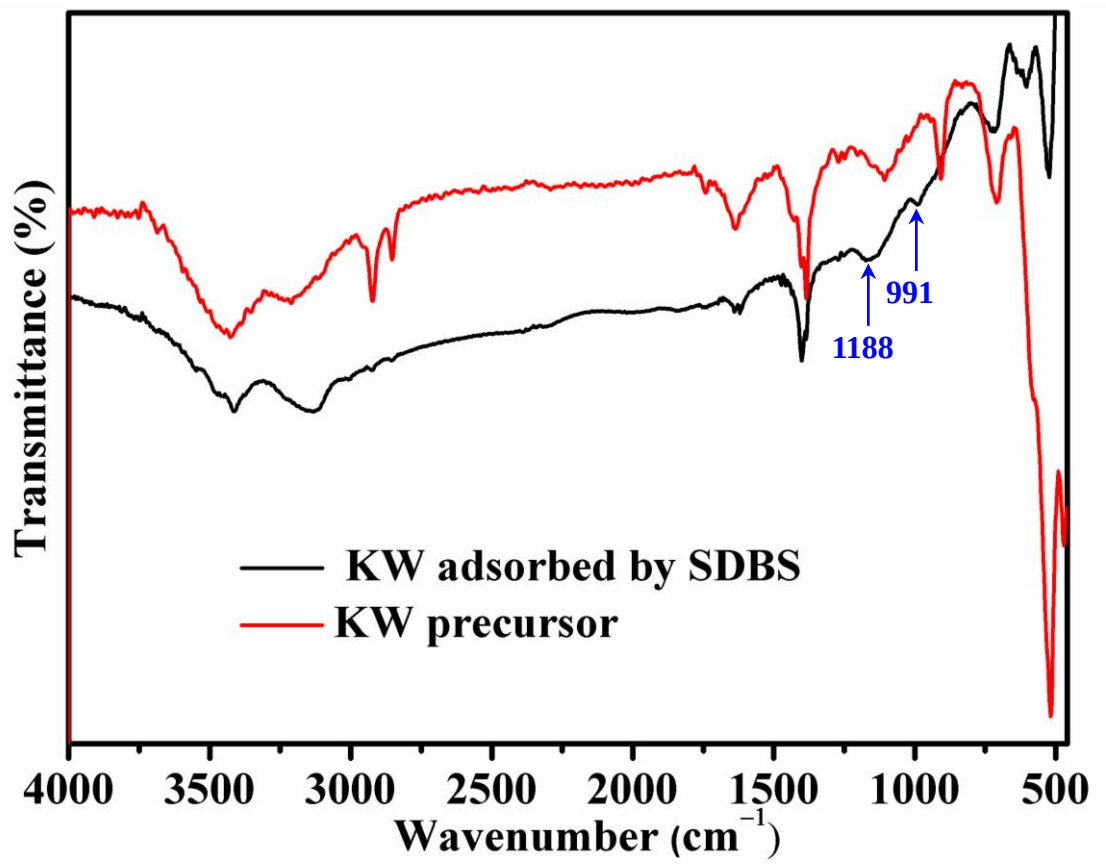

Fig. S3 FTIR spectra of KWs before and after adsorption of SDBS.

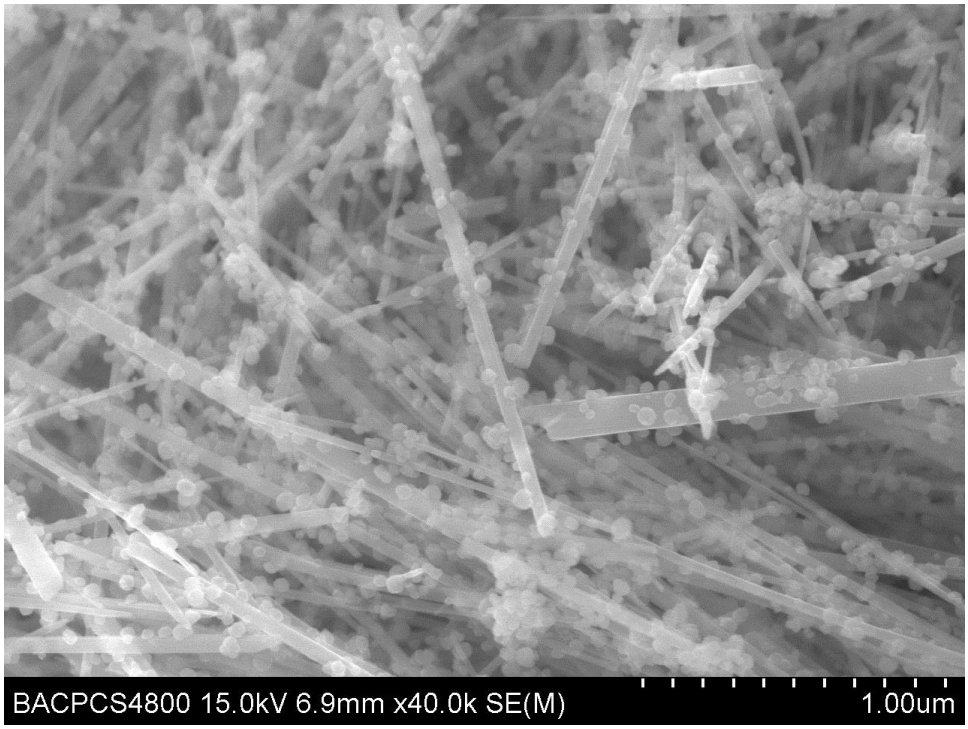

Fig. S4 SEM image of the products obtained by hydrothermal treatment of 0.05 g KW in 10 mL 0.1 M $Fe(NO_3)_3$ aqueous solution at 170–180 °C for 36 h.

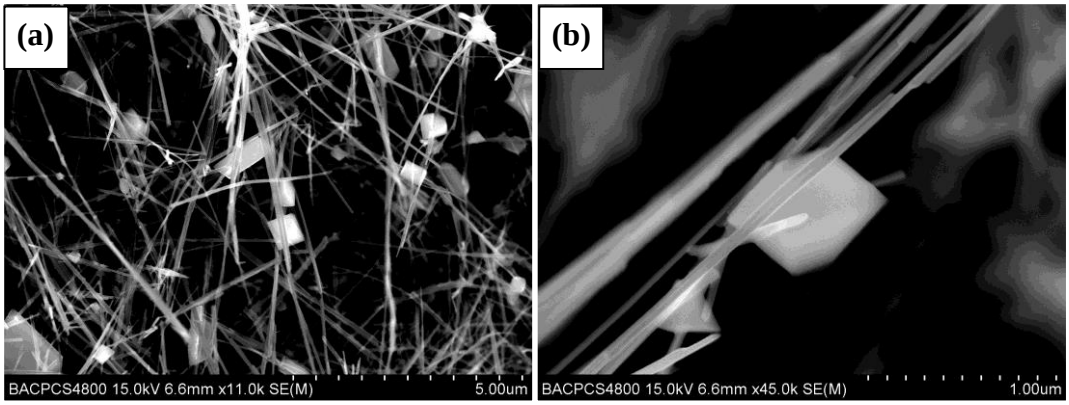

Fig. S5 SEM images of the products obtained by hydrothermal treatment of 0.05 g KW in 10 mL 0.07 M $Co(NO_3)_3$ aqueous solution at 150–160 °C for 24 h.

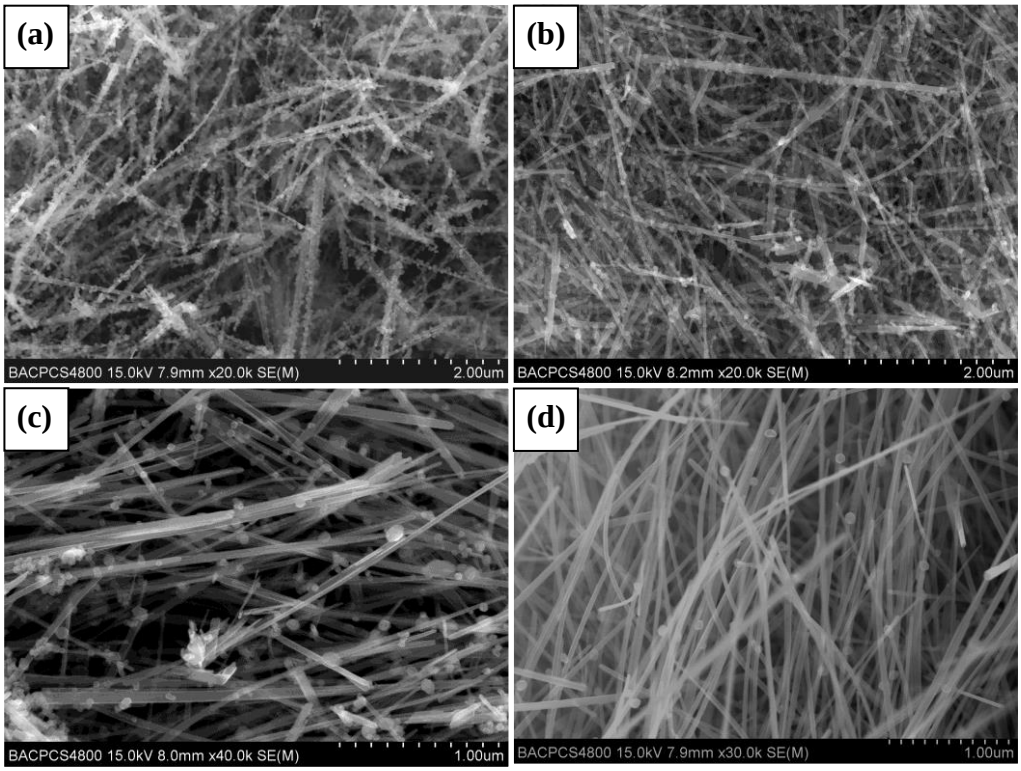

Fig. S6 SEM images of the products obtained by hydrothermal treatment of 0.05 g KW in 10 mL $Fe(NO_3)_3$ aqueous solution with different concentration at 150–160 °C for 24 h. (a) 0.08 M, (b) 0.06 M, (c) 0.04 M, (d) 0.02 M.

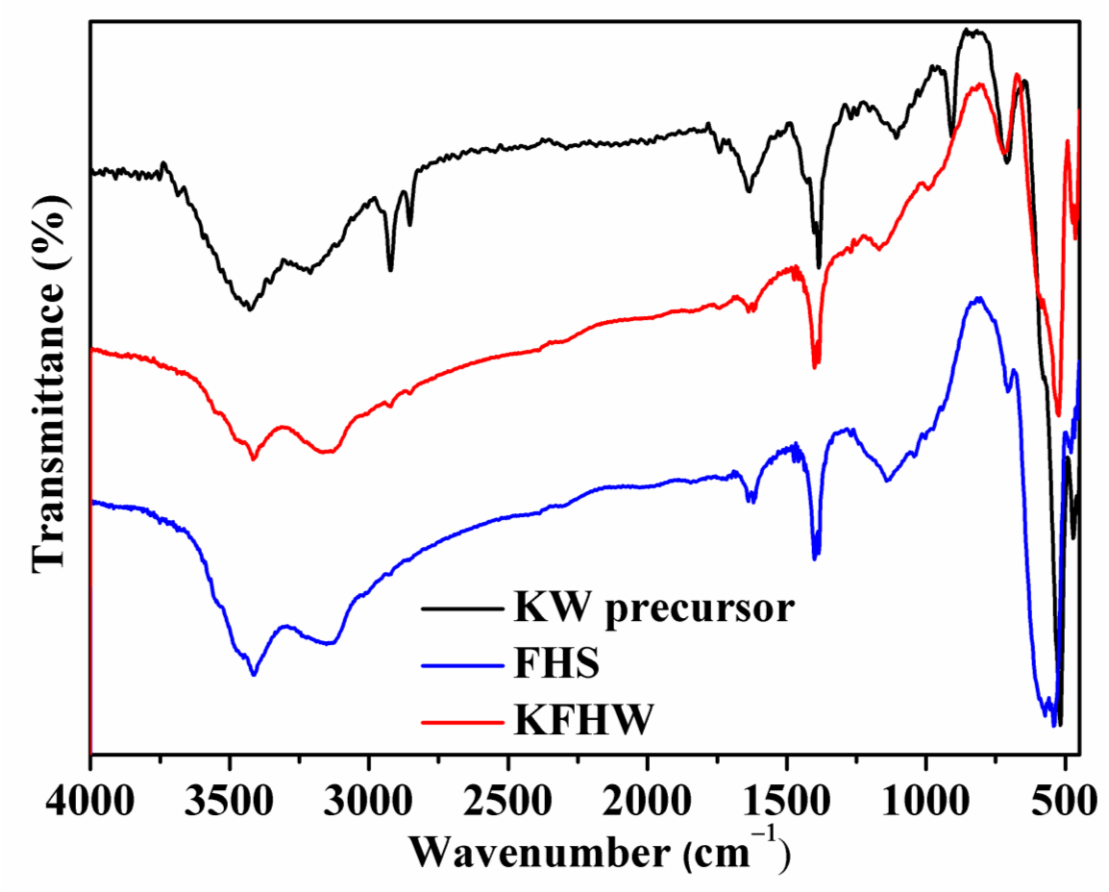

Fig. S7 FTIR spectra of KW precursor, as-prepared FHS and KFHW nanostructures, showing the presence of hydroxyl groups on their surface. The broad, intense band at 3412 cm^{-1} is ascribed to the stretching of O–H.

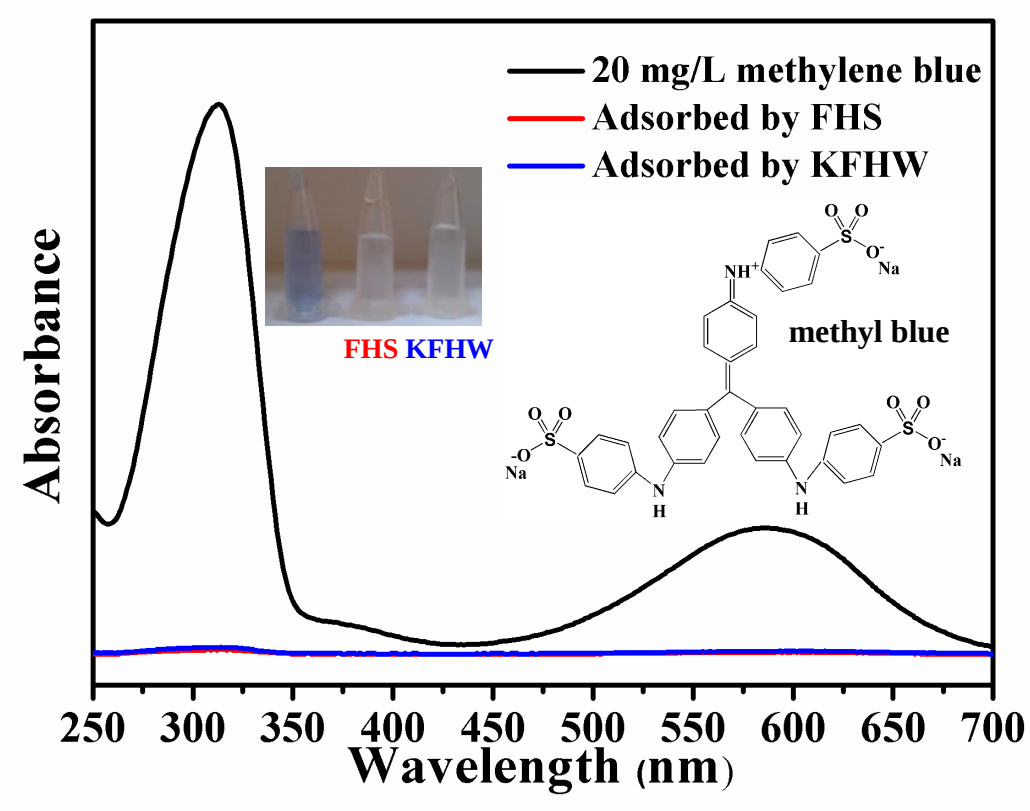

Fig. S8 UV-vis absorption spectra and optical image of methyl blue dye before (10 mL, 20 mg/L, black curve) and after (red and blue curves) adsorption treatment for 720 min with 20 mg as-prepared FHS and KFHW nanostructures.

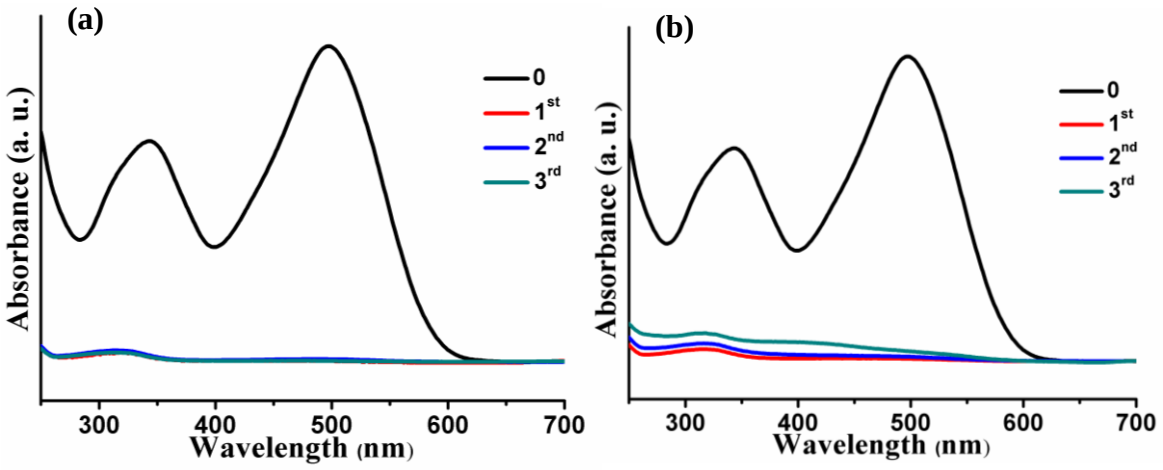

Fig. S9 Adsorption performance of FHS (a) and KFHW (b) toward 80 mg/L Congo red solution within three cycles.

Table S1. Pseudo first-order kinetic parameters for the adsorption of Congo red onto KFHWs and FHSs at various initial dye concentrations.

C_0 (mg/L)	K_1 (g/(mg·min))		$q_{e,exp}$ (mg/g)		$q_{e,cal}$ (mg/g)		R^2	
	KFHW	FHS	KFHW	FHS	KFHW	FHS	KFHW	FHS
20	0.0007711	-	9.94695	10.00000	0.03304	-	-0.14794	-
40	0.0338310	0.004053	19.92434	20.00000	0.05990	0.301835	0.57184	0.88766
80	0.0045599	0.004399	39.80523	39.92696	1.24741	0.27522	0.98682	0.54221
120	0.0035466	0.004767	59.14460	59.02260	1.00774	1.075895	0.65452	0.94780
160	0.0052738	0.004353	71.48387	77.35520	6.95792	7.397415	0.8331	0.44797
200	0.0029708	0.002925	85.56701	96.66300	22.56420	7.837364	0.61552	0.27737

Table S2. Pseudo second-order kinetic parameters for the adsorption of Congo red onto KFHWs and FHSs at various initial dye concentrations.

C_0 (mg/L)	K_2 (g/(mg·min))		$q_{e,exp}$ (mg/g)		$q_{e,cal}$ (mg/g)		R^2	
	KFHW	FHS	KFHW	FHS	KFHW	FHS	KFHW	FHS
20	0.53448	-	9.94695	10.00000	9.94431	10.00000	1.00000	1.00000
40	0.65065	0.10629	19.92434	20.00000	19.92826	20.00000	1.00000	1.00000
80	0.02524	0.13553	39.80523	39.92696	39.80892	39.92016	0.99998	1.00000
120	0.03065	0.03066	59.14460	59.02260	59.13661	59.03188	0.99999	1.00000
160	0.00509	0.00485	71.48387	77.35520	71.53076	77.27975	0.99989	0.99982
200	0.00103	0.003461	85.56701	96.66300	85.25149	96.43202	0.99647	0.99967

Table S3. The intra-particle diffusion constants for Congo red onto KFHWs and FHSs at different initial concentrations.

C_0 (mg/L)	k_{in} (mg/g $min^{1/2}$)		C		R^2	
	KFHW	FHS	KFHW	FHS	KFHW	FHS
20	0.00139	0.00011	9.90425	10	0.98136	0.99998
40	0.00824	0.01197	19.71326	19.69211	0.98133	0.95010
80	0.05337	0.01459	38.45699	39.55701	0.97143	0.92106
120	0.03600	0.04029	58.18495	57.98704	0.96013	0.98197
160	1.90584	2.70869	57.27117	58.57780	0.98204	0.90807
200	5.51365	3.02468	40.93999	76.40128	0.93320	0.85011

Table S4. Langmuir isotherm fitting parameters for Congo red onto KFHWs and FHSs.

KFHWs			FHSs		
q_m (mg/g)	K_L (L/g)	R^2	q_m (mg/g)	K_L (L/g)	R^2
84.53085	1.32327	0.98932	93.54537	2.68593	0.96308

Table S5. Adsorption capacities of Congo red dye on various adsorbents.

Adsorbent	**Isotherm**	**Adsorbent capacity (mg/g)**	**Reference**
Acid-treated pine cone	Freundlich	40.2	1
Cashew nut shell	Langmuir	5.2	2
$Fe_{2.95}La_{0.05}O_4$ nanoparticles	Langmuir	107.6	3
γ-Fe_2O_3 nanoparticles	Langmuir	208.3	4
Mesoporous Fe_2O_3	-	53.0	5
Flower-like chain Nickel	-	59.2	6
$MnFe_2O_4$ octahedra nanoparticles	Langmuir	92.4	7
Magnetic core-manganese oxide shell nanoparticles	-	42.0	8
Magnetic cellulose/Fe_3O_4/activated carbon composite	Langmuir	66.1	9
Ball-milled sugarcane bagasse	Freundlich	38.2	10
FHS	Langmuir	93.5	This study
KFHW	Langmuir	84.5	This study

References:

1. S. Dawood and T. K. Sen, *Water Res.*, 2012, **46**, 1933–1946.

2. P. S.Kumar, S. Ramalingam, C. Senthamarai, M. Niranjanaa, P. Vijayalakshmi, S.

Sivanesan, *Desalination*, 2010, **261**, 52–60.

3. L. Wang, J. Li, Y. Wang and L. Zhao, *J. Hazard. Mater*., 2011, **196**, 342–349.

4. A. Afkhami and R. Moosavi, *J. Hazard. Mater*., 2010, **174**, 398–403.

5. C. Yu, X. Dong, L. Guo, J. Li, F. Qin, L. Zhang, J. Shi, D. Yan, *J. Phys. Chem. C*, 2008, **112**, 13378–13382.

6. G. Zhang and L. Zhao, *Dalton Trans.*, 2013, **42**, 3660–3666.

7. L. Wang, J. Li, Y. Wang, L. Zhao and Q. Jiang, *Chem. Eng. J.*, 2012, **181–182**, 72–79.

8. Y. Zhai, J. F. Zhai, M. Zhou and S. J. Dong, *J. Mater. Chem.*, 2009, **19**, 7030–7035.

9. H. Y. Zhu, Y. Q. Fu, R. Jiang, J.H. Jiang, L. Xiao, G. M. Zeng, S. L. Zhao and Y. Wang, *Chem. Eng. J.*, 2011, **173**, 494–502.

10. Z. Zhang, L. Moghaddam, I. M. O'Hara and W. O. S. Doherty, *Chem. Eng. J.*, 2011, **178**, 122–128.

Table S6. Freundlich isotherm parameters for Congo red onto KFHWs and FHSs.

KFHWs			FHSs		
K_F (L/g)	n	R^2	K_F (L/g)	n	R^2
56.61930	7.96432	0.88883	62.70806	4.62257	0.94253

Table S7. Parameters for ploting Dubinin-Radushkevich adsorption isotherm of Congo red onto KFHWs and FHSs (T=293 K).

KFHWs			FHSs		
q_s (mg/g)	K_{ad} (mol^2/KJ^2)	R^2	q_s (mg/g)	K_{ad} (mol^2/KJ^2)	R^2
78.04144	$2.57744*10^{-7}$	0.67906	89.75287	$1.36012*10^{-7}$	0.81081

Method:

Dubinin-Radushkevich isotherm is generally applied to express the adsorption mechanism with a Gaussian energy distribution onto a heterogeneous surface, and also is chosen to estimate the characteristic porosity and the apparent energy of adsorption.[1, 2] The model has often successfully fitted high solute activities and the intermediate range of concentrations data well. Dubinin-Radushkevich equation is given by [2–4]

$$\ln q_e = \ln q_s - K_{ad}\varepsilon^2$$

where q_e, q_s, K_{ad}, and ε are the amount of adsorbate in the adsorbent at equilibrium (mg/g), theoretical isotherm saturation capacity (mg/g), Dubinin-Radushkevich isotherm constant (mol^2/kJ^2), and the polyani potential, respectively. The parameter ε can be calculated by using[5, 6]

$$\varepsilon = RT\ln\left(1+\frac{1}{Ce}\right)$$

where R, T and C_e represent the gas constant (8.314 J/mol K), absolute temperature (K) and adsorbate equilibrium concentration (mg/L), respectively. The slope of these plots of $\ln q_e$ versus ε^2 gives K_{ad} and the intercept yields the adsorption capacity q_s. The

calculated results are given in **Table S7**, indicating that the adsorption kinetics does not follow Dubinin-Radushkevich isotherm model due to the low R^2 values.

1. V. Guptha, J. Agarwal, M. Purohit and Veena, *Res. J. Chem. Environ.*, 2007, **1191**, 40–43

2. A. O. Dada, A. P. Olalekan, A. M. Olatunya and O. DaDa, *J. Applied. Chem.*, 2012, **3**, 38–45.

3. A. Gunay, E. Arslankaya and I. Tosun, *J. Hazard. Mater.*, 2007, **2146**, 362–371.

4. A. Dabrowski, *Adv. Colloid Interface Sci.*, 2001, **93**, 135–224.

5. M. M. Dubinin, *Chem. Rev.*, 1960, **60**, 235–266.

6. J. P. Hobson, *J. Phys. Chem*., 1969, **73**, 2720–2727.